Nesfatin-1 Action in the Brain Increases Insulin Sensitivity Through Akt/AMPK/TORC2 Pathway in Diet-Induced Insulin Resistance

Mengliu Yang,[1] Zhihong Zhang,[1] Chong Wang,[1] Ke Li,[1] Shengbing Li,[1] Guenther Boden,[2,3] Ling Li,[1] and Gangyi Yang[1]

Nesfatin-1, derived from nucleobindin 2, was recently identified as an anorexigenic signal peptide. However, its neural role in glucose homeostasis and insulin sensitivity is unknown. To evaluate the metabolic impact and underlying mechanisms of central nesfatin-1 signaling, we infused nesfatin-1 in the third cerebral ventricle of high-fat diet (HFD)–fed rats. The effects of central nesfatin-1 on glucose metabolism and changes in transcription factors and signaling pathways were assessed during euglycemic-hyperinsulinemic clamping. The infusion of nesfatin-1 into the third cerebral ventricle markedly inhibited hepatic glucose production (HGP), promoted muscle glucose uptake, and was accompanied by decreases in hepatic mRNA and protein expression and enzymatic activity of PEPCK in both standard diet- and HFD-fed rats. In addition, central nesfatin-1 increased insulin receptor (InsR)/insulin receptor substrate-1 (IRS-1)/AMP-dependent protein kinase (AMPK)/Akt kinase (Akt)/target of rapamycin complex (TORC) 2 phosphorylation and resulted in an increase in Fos immunoreactivity in the hypothalamic nuclei that mediate glucose homeostasis. Taken together, these results reveal what we believe to be a novel site of action of nesfatin-1 on HGP and the PEPCK/InsR/IRS-1/AMPK/Akt/TORC2 pathway and suggest that hypothalamic nesfatin-1 action through a neural-mediated pathway can contribute to increased peripheral and hepatic insulin sensitivity by decreasing gluconeogenesis and promoting peripheral glucose uptake in vivo. *Diabetes* 61:1959–1968, 2012

See accompanying commentary, p. 1920.

Energy and metabolic homeostasis depend on signals from endocrine, neural, and metabolic origins. Among the regulatory signals, neuropeptides generated by the central nervous system play an essential role in the regulation of food intake and energy expenditure (1–3). The hypothalamus is emerging as a critical site for the integration of nutritional, endocrine, and neural cues, generating signals that activate feedback loops between nutrient intake and metabolism (4–9). Therefore, it is likely that hypothalamic signals will affect changes in weight and insulin sensitivity. In fact, behavioral and metabolic effects of hypothalamic factors have been reported in various animal models of diet-induced insulin resistance (10–13).

Nesfatin-1 is an 82-amino acid protein derived from nucleobindin 2 (NUCB2), which is highly conserved in mammalian species. Nesfatin-1 is distributed not only throughout the brain, but also in peripheral tissues (14–16). An initial report suggested that nesfatin-1 may be a physiological regulator of food intake. Nesfatin-1 injected intracerebroventricularly (ICV) in rats reduced body weight, whereas injection of the antisense oligonucleotide against the gene encoding NUCB2 increased body weight (14). Recent studies have demonstrated that the expressions of NUCB2 mRNA and nesfatin-1 protein were regulated by cytokines in 3T3-L1 cells and adipose tissue explants (17). Furthermore, circulating and adipose tissue levels of nesfatin-1 protein were elevated in obese mice, whereas human plasma nesfatin-1 levels correlated positively with increasing BMI (17). These findings supported a role of nesfatin-1 in the regulation of energy homeostasis. However, there are no reports on the effects of central administration of nesfatin-1 on glucose homeostasis and insulin sensitivity, nor has the signaling pathway of central nesfatin-1 action been identified. Therefore, the aim of this study was to examine the effects of ICV nesfatin-1 on glucose metabolism, and nesfatin-1 signaling, particularly its involvement in the insulin receptor (InsR)/insulin receptor substrate 1 (IRS-1)/AMP-dependent protein kinase (AMPK)/Akt kinase (Akt)/mammalian target of rapamycin (mTOR) pathway.

RESEARCH DESIGN AND METHODS

Animals. Male Sprague-Dawley rats weighing between 120 and 130 g (Animal Center of Chongqing Medical University, Chongqing, China) were studied. Rats were randomly divided into two groups and fed either a standard diet (SD; 59% calories from carbohydrates) or a high-fat diet (HFD; 53% of calories from fat) for 10 weeks. All experimental procedures were approved by the Animal Experimentation Ethics Committee (Chongqing Medical University). Ten days before the in vivo studies, rats were equipped with chronic catheters placed into the third cerebral ventricle. Briefly, animals were anesthetized with intraperitoneal ketamine (87 mg/kg) and fixed in a stereotaxic apparatus. A 26-gauge stainless steel guide cannula was implanted into the third ventricle. A 28-gauge dummy cannula was inserted to prevent clogging of the guide cannula. The implant was secured to the skull with Caulk Grip dental cement (Dentsply International Inc., York, PA), and the skin was closed over the implant using wound clips. After confirming the correct cannula placement by testing the drinking response to angiotensin II, rats received sham ICV injections for 2 days. After 7 days, rats were anesthetized with intraperitoneal pentobarbital (50 mg/kg), and indwelling catheters were inserted into the right internal jugular vein and left carotid artery for infusion or blood sampling, respectively. After this, animals were allowed to recover for 3 days (18).

ICV studies. To determine the role of central nesfatin-1, we performed ICV infusions of nesfatin-1 (25 pmol; Phoenix Pharmaceuticals, Belmont, CA) or artificial cerebrospinal fluid (ACF) at a rate of 6 μL/h for 6 h. ICV infusions were started 120 min before the beginning of the euglycemic-hyperinsulinemic

clamps (EHC) and continued throughout the study. Four treatment groups were studied: *1*) SD–ACF (NCA group; *n* = 10); *2*) SD–nesfatin-1 (NCN group; *n* = 10); *3*) HFD–ACF (HFA group; *n* = 10); and *4*) HFD–nesfatin-1 (HFN group; *n* = 10); All rats underwent EHC during the last 2 h of infusion (Fig. 1*A*).

EHC studies. After a 12-h fast, EHC were performed in conscious, catheterized rats as described (19). Briefly, at *t* = 120 min, a primed, continuous infusion of high-performance liquid chromatography-purified [^{3}H-3]glucose (Amersham, Los Angeles, CA; 6 μCi bolus, 0.2 μCi/min) was initiated and continued for the 4 h. At 240 min, a continuous infusion of insulin (6 mU · kg^{-1} · min^{-1}) and a variable infusion of 25% glucose to maintain the plasma glucose concentration at ~6 mmol/L was administered. Blood samples (100 μl) were obtained from the jugular vein catheter at −120, 0, 120, 180, 200, 210, and 220 min for determination of insulin, free fatty acids (FFA), or glucose-specific activity. Forty-five minutes before the end of the infusion studies, 2-deoxy-D-[^{3}H]glucose (2-DG; Amersham; 2 μCi bolus) was administered to determine insulin-mediated glucose uptake in individual tissues. Extra blood samples (50 μl) were taken at 2, 5, 10, 15, 20, 30, and 45 min after the injection to determine the tracer disappearance curve. At the end of the clamp, the rats were anesthetized, and tissue samples were freeze-clamped in situ with aluminum tongs precooled in liquid nitrogen and stored at −80°C for subsequent analysis (Fig. 1*B*).

RNA extraction and quantitative real-time RT-PCR. We obtained total RNA from frozen tissue with TRIzol reagent (Invitrogen) according to the manufacturer's instructions. Quantitative real-time RT-PCR was performed with a SYBR Green PCR kit (Takara Bio, Otsu, Japan), and a Corbett Rotor Gene 6000 real-time PCR system (Corbett Research, Sydney, Australia) according to the manufacturer's instructions. Gene expressions were analyzed using the comparative threshold cycle method and normalized with β-actin. The following sequences of the primers were used: 5′-CCCTGAACCCTAAGGCCAACCGT-GAAAA-3′ and 5′-TCTCCGGAGTCCATCACAATGCCTGTG-3′ for β-actin; 5′-CACCTTGACAC TACACCCTT-3′ and 5′-GTGGCTGTGAACACCTCT-3′ for glucose-6-phosphatase (*G-6-Pase*); and 5′-AGTCACCATCACTTCCTGGAAGA-3′ and 5′-GGTGCAGAATC GCGAGTT-3′ for *PEPCK*.

Western blot analyses. Liver tissues were homogenized, and protein concentration was measured with a BCA protein quantification kit (Pierce Biotechnology). One microliter aliquot of tissue extracts (70 μg) was separated by SDS-polyacrylamide gel electrophoresis and transferred to polyvinylidene difluoride membranes. Immunoblots were then blocked in Tris-buffered saline containing 0.1% Tween-20 (TBST) and 5% skimmed milk overnight at 4°C and incubated with primary antibodies including G-6-Pase, PEPCK (Santa Cruz Biotechnology), InsR, phospho-InsR, IRS-1, phospho–IRS-1, Akt, phospho-Akt, AMPK, phospho-AMPK, mTOR, phospho-mTOR (Cell Signaling Technology), the mammalian target of rapamycin complex 2 (TORC2), phospho-TORC2, and β-actin (Research Diagnostics) (1:500 dilution) for 2 h at room temperature. Following three consecutive 5-min washes in TBST, blots were incubated with horseradish peroxidase-conjugated secondary antibody (Invitrogen) (1:500 dilution) for 1 h at room temperature. After two washes in TBST and a final wash in TBS, the blots were scanned using the Odyssey Infrared Imaging System (LI-COR Biosciences), and quantification of antigen–antibody complexes was performed using Quantity One analysis software (Bio-Rad).

Measurement of hepatic glucose-regulating enzyme activities. A total of 200 mg of freeze-clamped liver was powderized and homogenized by sonication in 0.25 mol/L sucrose and 10 mmol/L *N*-2-hydroxyethylpiperazine-*N*′-2-ethanesulfonic acid (pH 7.4). G-6-Pase and PEPCK activity were assayed as described by Thomas et al. (20). The glucokinase (GK) activity was determined based from the method of Davidson (21) with slight modification.

Fos immunohistochemistry. Nesfatin-1 or ACF was injected ICV in rats. Three hours later, the rats were anesthetized with pentobarbital and perfused with saline containing heparin (20 U/ml) for 3 min and then 4% paraformaldehyde in 0.1 M PBS for 20 min.

The brains were excised, transferred to 4% paraformaldehyde, and then fixed at 4°C for 24 h. After being dehydrated through an ethanol-xylene series, the specimens were embedded in paraffin and coronal sections of the hypothalamus. Immunohistochemistry for Fos protein (rabbit anti-c-Fos, 1:10,000; Oncogene, Cambridge, MA) was performed as described previously (22).

Analytical procedures. [3-^{3}H]Glucose and 2-DG radioactivities were determined by scintillation counter. Plasma FFA was determined spectrophotometrically using an acyl-CoA oxidase-based colorimetric kit (Wako Pure Chemical Industries, Osaka, Japan). Insulin and ghrelin were measured using a commercial insulin enzyme-linked immunosorbent assay kit (Diagnostic Products, Los Angeles, CA; Phoenix Pharmaceuticals, Belmont, CA). Plasma glucagon levels were determined using an RIA kit (Bad Nauheim, Germany). Plasma glucose was measured using the glucose oxidase method. Triacylglycerol (TG), total cholesterol (TC), HDL cholesterol (HDL-C), and LDL cholesterol (LDL-C) concentrations were measured using enzymatic colorimetric kits. Hepatic glycogen levels were measured using glycogen assay kits (BioVision, Mountain View, CA).

Statistical analysis. All results are expressed as means ± SEM. A two-way ANOVA with a least significant difference post hoc test was used to compare mean values between multiple groups and a two-sample, unpaired Student *t* test was used for two-group comparisons.

RESULTS

Central nesfatin-1 increases whole-body insulin sensitivity in HFD rats. The mean body weights were significantly higher in HFD rats than in SD rats. Similarly, following, a 12-h fast, plasma insulin, TG, TC, LDL-C, HDL-C, and FFA concentrations were higher in HFD rats compared with SD rats (Supplementary Table 1). Two-way ANOVA analysis indicated that HFD feeding but not central nesfatin-1 altered glucose, TC, LDL-C, HDL-C, and FFA in these rats (Table 1) and that both diet and central nesfatin-1 affected the insulin, TG, and glucose infusion rates (GIR) during the EHC (Table 1). During EHC, FFA and TG were significantly suppressed in all groups, but remained higher in HFD than in SD rats (Table 1). In SD-fed rats, nesfatin-1 increased the GIR required to prevent changes in the plasma glucose levels (28.3 ± 1.4 vs. 23.0 ± 1.7 mg/kg/min, nesfatin-1 vs. ACF; *P* < 0.01) (Fig. 1*C*). As expected, HFD-fed rats developed insulin resistance so that less glucose had to be infused during the clamp procedure (10.1 ± 1.6 vs. 23.0 ± 1.7 mg/kg/min; *P* < 0.01). ICV infusion of nesfatin-1 markedly increased GIR in HFD rats (17.8 ± 2.1 vs. 10.1 ± 1.6 mg/kg/min; *P* < 0.01) (Fig. 1*C*). Whole-body glucose uptake was slightly increased in both SD and HFD rats with nesfatin-1 compared with ACF infusion (Fig. 1*D*). As circulating food intake-related factors might be regulated by the central nesfatin-1, we examined plasma ghrelin, an orexigenic hormone, levels before and the end of the clamps. Preclamp ghrelin levels were similar in HFD rats with or without central nesfatin-1. At the end of the clamps, plasma ghrelin was suppressed similarly by hyperinsulinemia (ACF: from 842.2 ± 92.4 to 698.5 ± 88.9 μg/L; nesfatin-1: from 885.4 ± 78.6 to 738.7 ± 102.3 μg/L; both *P* < 0.05), showing that short-term ICV nesfatin-1 did not affect ghrelin secretion.

Central nesfatin-1 increases hepatic insulin action in HFD-fed rats. Central nesfatin-1 significantly increased the ability of insulin to suppress hepatic glucose production (HGP) in SD-fed rats (6.67 ± 0.33 vs. 8.81 ± 2.93 mg/kg/min, nesfatin-1 vs. ACF; *P* < 0.05) (Fig. 1*E*). In HFD-fed rats, insulin's ability to suppress HGP was significantly impaired (15.33 ± 2.67 vs. 8.81 ± 2.93 mg/kg/min, HFD vs. SD; *P* < 0.01) (Fig. 1*E*), confirming the presence of hepatic insulin resistance. The ICV nesfatin-1 restored hepatic insulin action to normal in HFD rats (Fig. 1*E*). The action of insulin on glucose production can also be expressed as percent suppression from basal levels (Fig. 1 F). However, because plasma insulin was not similar in all groups, we calculated the GIR per plasma insulin ratio in each individual. This ratio, an index of insulin action, was reduced in HFD-fed rats and increased by nesfatin-1 (Fig. 1*G*), confirming the presence of insulin resistance and central nesfatin-1–mediated insulin sensitization. To examine whether the effect of central nesfatin-1 on HGP is secondary to decreased glucagon, we assessed plasma glucagon levels in SD–ACF and SD–nesfatin-1 rats. At the end of the clamp, glucagon levels were similar in the two groups (40.5 ± 2.6 vs. 38.8 ± 3.8 ng/L), suggesting that central nesfatin-1 failed to affect glucagon release. Due to high-energy diet, the HFD-fed rats showed significantly decreased hepatic glycogen stores compared with SD-fed rats

FIG. 1. Central nesfatin-1 administration increases insulin sensitivity in HFD-fed rats. Male Sprague-Dawley rats received implantation of ICV cannulae on day 0 (10 days before the in vivo study) and venous and arterial catheters on day 7. Following recovery from the surgery (day 10), rats were divided into four groups: NCA, NCN, HFA, and HFN. *A*: Experimental protocol for catheter implantation. *B*: EHC. Rats received ICV infusion of nesfatin-1 or vehicle (ACF) before and during the in vivo experiments. At 120 min, an infusion of [³H-3]glucose was initiated. The clamp procedure started at 240 min. This involved the infusion of insulin (6 mU/kg/min) and glucose (as needed to prevent hypoglycemia). *C*: GIR. *D*: The rate of glucose disposal (GRd). *E*: HGP. *F*: Percentage suppression of endogenous glucose production induced by insulin infusion. *G*: The ratio of GIR (mg/kg/min) to insulin (kg/min/mU) during clamps. The mean of 10 rats per group is shown. *$P < 0.05$, **$P < 0.01$ vs. NCA group, ▲$P < 0.05$, ▲▲$P < 0.01$ vs. HFA group.

TABLE 1
Plasma parameters and glucose infusion rate during the hyperinsulinemic clamp studies

Treatment	SD rats		HFD rats		Two-way ANOVA (P values)		
	ACF	Nesfatin-1	ACF	Nesfatin-1	Diet	Treatment	Diet × Treatment
Glucose (mmol/L)	5.45 ± 0.16	5.49 ± 0.23	5.20 ± 0.31	5.20 ± 0.24	0.001	0.813	0.777
Insulin (mU/L)	99.03 ± 2.01	100.90 ± 2.65	139.26 ± 39.32*	100.42 ± 13.25	0.005	0.008	0.004
TC (mmol/L)	1.16 ± 0.04	1.14 ± 0.05	1.60 ± 0.31*	1.55 ± 0.26*	<0.001	0.539	0.790
TG (mmol/L)	0.16 ± 0.03	0.16 ± 0.03	0.68 ± 0.20*	0.48 ± 0.17*	<0.001	0.019	0.024
LDL-C (mmol/L)	0.56 ± 0.04	0.53 ± 0.04	0.79 ± 0.22*	0.70 ± 0.19*	<0.001	0.194	0.570
HDL-C (mmol/L)	0.95 ± 0.04	0.90 ± 0.08	0.76 ± 0.06†	0.78 ± 0.09†	<0.001	0.661	0.117
FFA (mmol/L)	0.22 ± 0.03	0.19 ± 0.02	0.69 ± 0.26*	0.55 ± 0.22*	<0.001	0.141	0.289
GIR (mg/kg/min)	23.03 ± 0.55	28.25 ± 0.45	10.07 ± 0.51*	17.76 ± 0.65*	<0.001	<0.001	0.030

Data are means ± SE. *$P < 0.01$, †$P < 0.05$ vs. SD plus ACF.

(Fig. 2A). Central nesfatin-1 failed to change glycogen level in both SD- and HFD-fed rats (Fig. 2A).

Central nesfatin-1 increases insulin-induced glucose uptake in muscle of HFD-fed rats. 2-DG was used as a nonhydrolyzable tracer injected during EHC to determine glucose uptake into muscle. The amount of 2-DG that accumulated in both soleus and gastrocnemius muscle of SD-fed rats was significantly higher with ICV nesfatin-1 infusion than with ACF infusion rats (soleus: 6.73 ± 1.16 vs. 4.81 ± 0.73 μmol/100 g/min, $P < 0.05$; gastrocnemius: 2.46 ± 0.18 vs. 1.70 ± 0.37 μmol/100 g/min, $P < 0.05$) (Fig. 2B). As expected, HFD rats displayed a significantly decreased 2-DG uptake in soleus and gastrocnemius muscle compared with SD-fed rats (soleus: 1.49 ± 0.14 vs. 4.81 ± 0.73 μmol/100 g/min, $P < 0.01$; gastrocnemius: 0.51 ± 0.10 vs. 1.70 ± 0.37 μmol/100 g/min, $P < 0.01$) (Fig. 2B). However, ICV nesfatin-1 markedly increased the rate of muscle glucose uptake in HFD-fed rats (soleus: 2.39 ± 0.42 vs. 1.49 ± 0.14 μmol/100 g/min, $P < 0.01$; gastrocnemius: 0.89 ± 0.22 vs. 0.51 ± 0.1 μmol/100 g/min, $P < 0.01$) (Fig. 2B).

Hepatic glucose-regulating enzyme activity. Central nesfatin-1 decreased hepatic PEPCK activity in both SD- and HFD-fed rats compared with controls (21.0 ± 0.3 vs. 10.7 ± 0.9 mU/mg for SD-fed rats; 27.3 ± 0.7 vs. 10.9 ± 0.8 for HFD-fed rats; all $P < 0.01$) (Fig. 3A), but did not alter hepatic G-6-Pase activity (14.9 ± 0.8 vs. 13.8 ± 0.8 mU/mg for SD rats; 15.2 ± 0.9 vs. 14.6 ± 0.7 mU/mg for HFD rats) (Fig. 3B). Hepatic GK activity failed to show significant differences between HFD- and SD-fed rats. However, central nesfatin-1 led to a slightly yet nonsignificant increase in GK activity (Fig. 3C).

PEPCK but not G-6-Pase mRNA and protein expression are reduced by central nesfatin-1 in the liver. We next evaluated whether central nesfatin-1 affected PEPCK and G-6-Pase mRNA and proteins in the liver. We found a significant decrease in hepatic PEPCK protein after central nesfatin-1 treatment in both SD and HFD rats (−38 and −49%, respectively; $P < 0.05$) (Fig. 4A). PEPCK mRNA expression was similarly affected in these rats (−39 for SD, and −40% for HFD, respectively; $P < 0.05$) (Fig. 4B). Surprisingly, G-6-Pase mRNA and protein expression were not affected in four groups under the same experimental conditions (Fig. 4C and D).

Central nesfatin-1 enhances hepatic insulin signaling. In order to delineate the mechanisms by which central nesfatin-1 modulates glucose homeostasis, we assessed the effects of central nesfatin-1 on the phosphorylation of several proteins in the InsR → IRS-1 → AMPK → Akt signaling
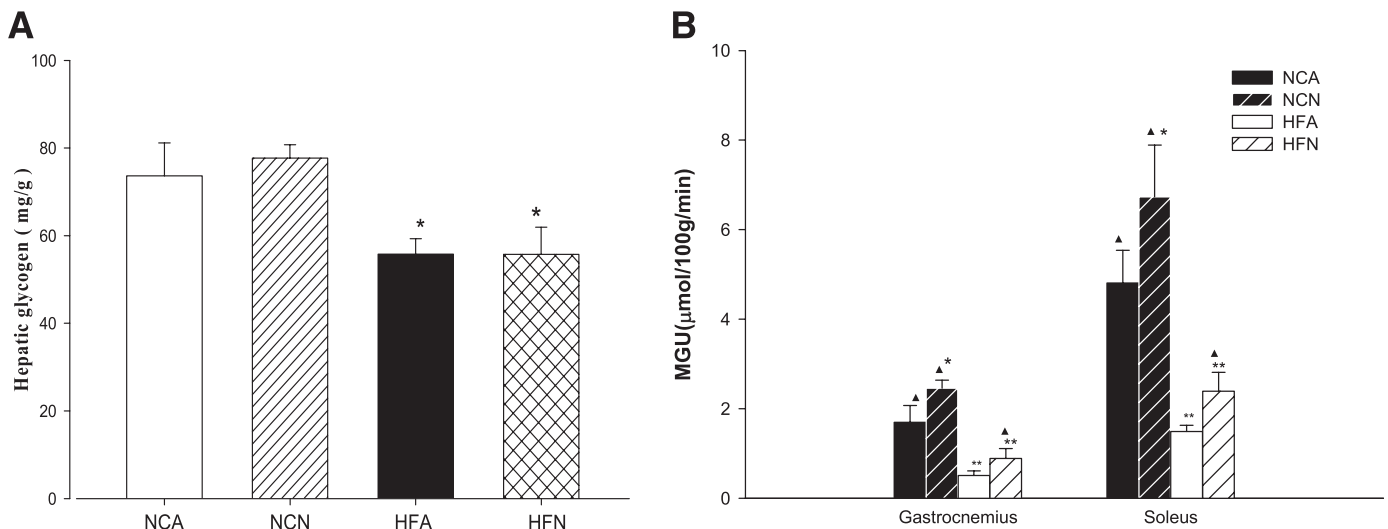

FIG. 2. The effects of central nesfatin-1 on individual tissue glucose uptake and hepatic glycogen. A: Hepatic glycogen. B: Muscle glucose uptake. Four treatment groups were studied: NCA, NCN, HFA, and HFN. Shown are means of 10 rats per group. *$P < 0.05$, **$P < 0.01$ vs. ICV ACF-infused rats (NCA), ▲$P < 0.01$ vs. HFD-fed rats (HFA).
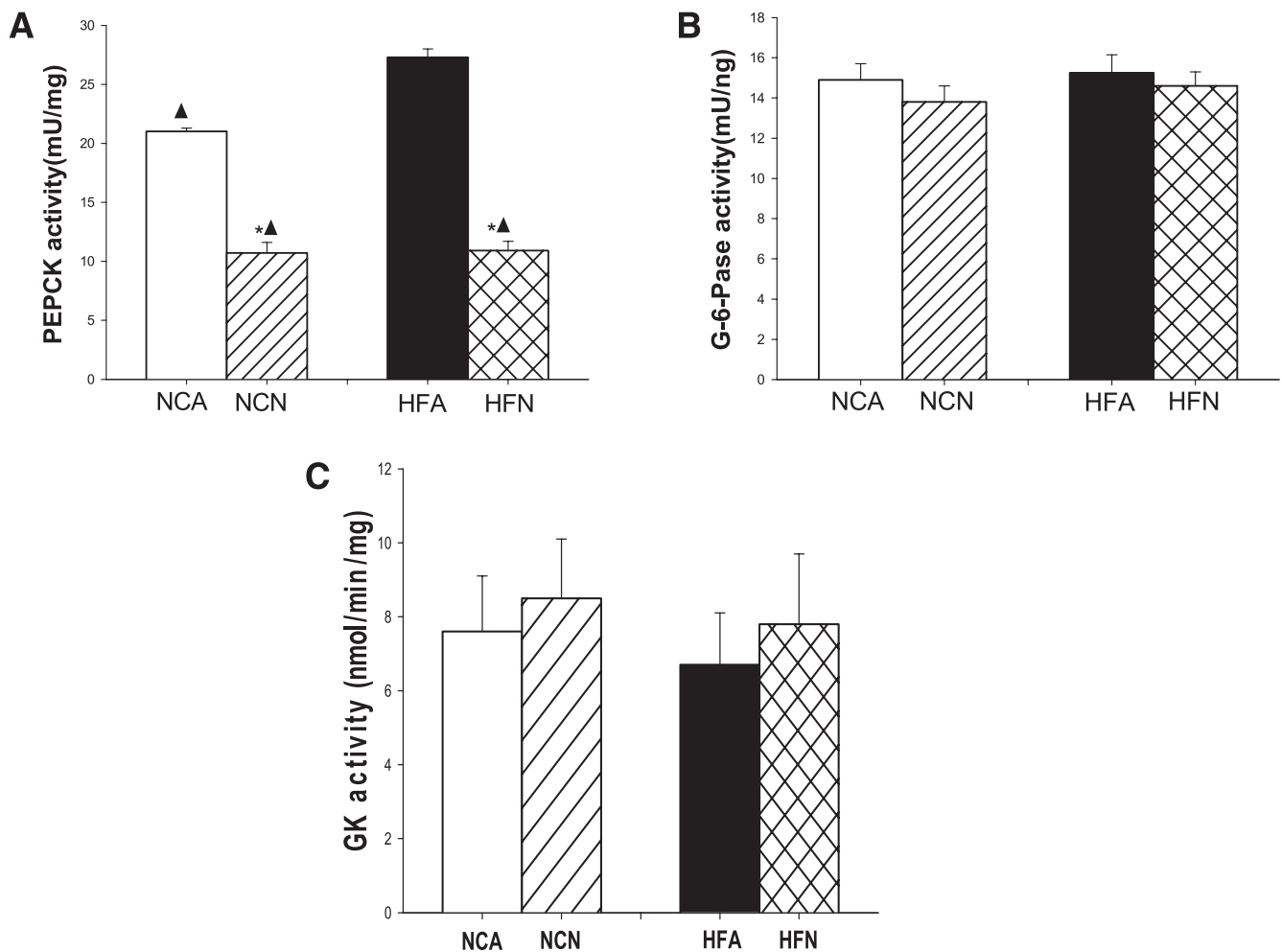
FIG. 3. The effect of central nesfatin-1 administration on the hepatic glucose-regulating enzyme activities. Four treatment groups were studied: NCA, NCN, HFA, and HFN. A: PEPCK activity. B: G-6-Pase activity. C: GK activity. Shown are means ± SE. *$P < 0.05$ vs. ICV ACF-infused rats (NCA), ▲$P < 0.05$ vs. HFD-fed rats (HFA).

cascade by immunoprecipitation followed by Western blots. Central nesfatin-1 significantly increased Tyr phosphorylation of InsR and IRS-1 in the liver of both SD and HFD rats (both $P < 0.05$) (Fig. 5A and B). We further examined the effect of central nesfatin-1 on Akt (Ser473) and AMPK (Thr172) phosphorylation in the liver of these rats. As shown in Fig. 5C and D, central nesfatin-1 led to a marked increase in the hepatic phosphorylation of AMPK (Thr172) and Akt (Ser473) in both SD and HFD rats. Immunoblot quantification revealed an increase of at least 1.2-fold (for SD rats) and 2.0-fold (for HFD rats) in the insulin-stimulated phosphorylation of AMPK (Thr172) compared with ACF-treated rats ($P < 0.05$ or $P < 0.01$) (Fig. 5A). However, as depicted in Fig. 5B, in SD rats, central nesfatin-1 only led to a nonsignificant slight increase hepatic Akt phosphorylation, whereas in HFD-fed rats, central nesfatin-1 caused a 0.8-fold increase in insulin-stimulated phosphorylation of Akt ($P < 0.05$) (Fig. 5D). These data demonstrate that central nesfatin-1 increases insulin sensitivity and glucose tolerance, in part, by sustained activation of the insulin-signaling pathway.

Central nesfatin-1 enhances TORC2 and mTOR phosphorylation. Because the mTOR complex pathway probably acts downstream of AMPK in the gluconeogenic

pathway, we also examined the effect of central nesfatin-1 on TORC2 (Thr171) and mTOR (Ser2448) phosphorylation in SD and HFD rats. As expected, HFD inhibited insulin-induced activation of TORC2 and mTOR, as shown by failure of insulin to increase phosphorylation in HFD rats compared with SD rats (Fig. 6A and B). However, with increasing Akt and AMPK activity, central nesfatin-1 resulted in enhanced phosphorylation of TORC2 (Thr171) (1.1- and 3.0-fold, respectively) and mTOR (Ser2448) (1.5- and 4.8-fold, respectively) in SD- and HFD-fed rats ($P < 0.05$ or $P < 0.01$) (Fig. 6A and B).

Central nesfatin-1 activates hypothalamic neurons. To examine whether the regulation of glucose homeostasis by central nesfatin-1 requires hypothalamic innervation, we performed a Fos analysis in hypothalamic centers known to impact on peripheral glucose metabolism. As shown in Fig. 7A and B, central nesfatin-1 led to a significant increase in the number of Fos-positive cells in the arcuate, paraventricular, and supraoptic nucleus, all of which have been implicated in glucose homeostasis. Therefore, immunohistochemical analysis confirmed that ICV nesfatin-1 stimulated glucose homeostasis-related neurons in the hypothalamic nuclei.
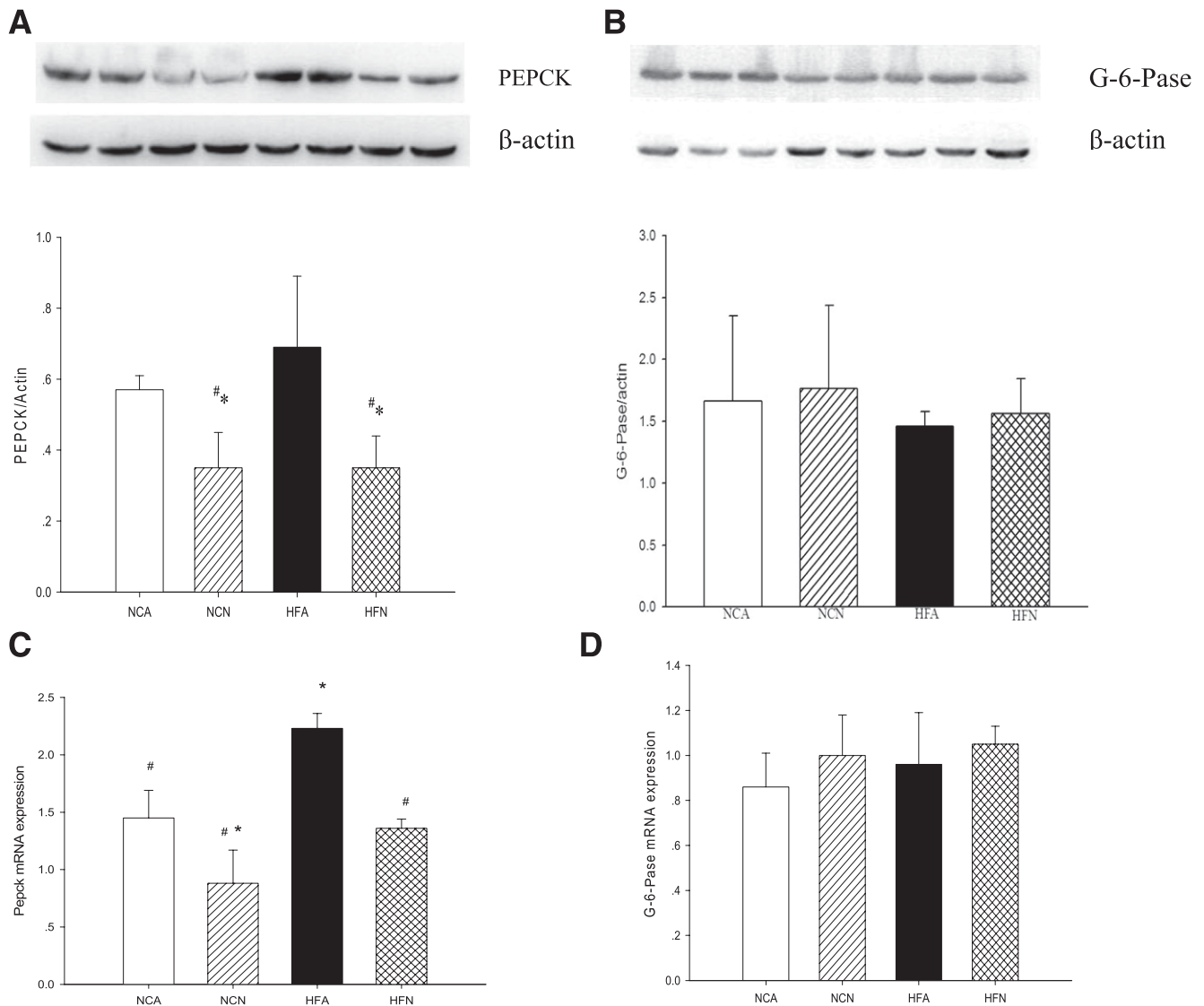
FIG. 4. The mRNA and protein expressions of PEPCK and G-6-Pase in the liver. Hepatic tissues were collected from four treatment groups—NCA, NCN, HFA, and HFN rats—and then immunoblotting or quantitative real-time PCR was performed as described in RESEARCH DESIGN AND METHODS. *A*: PEPCK protein abundance. *B*: G-6-Pase protein abundance. *C*: PEPCK mRNA expression. *D*: G-6-Pase mRNA expression. The graphs show the means ± SE from five independent experiments. The mRNA expression differences were normalized to a standard housekeeping mRNA level; data are presented as the relative expression. $*P < 0.05$ vs. ICV ACF-infused rats (NCA), $\#P < 0.05$ vs. HFD-fed rats (HFA).

DISCUSSION

There is growing evidence that nesfatin-1 may play an important role in the regulation of food intake and glucose homeostasis (1,23,24). For instance, continuous infusion of nesfatin-1 into the third brain ventricle significantly decreased food intake and body weight gain in rats (14). In previous studies, we have also shown that plasma nesfatin-1 levels were elevated in patients with type 2 diabetes mellitus (T2DM) and associated with BMI, plasma insulin, and the homeostasis model assessment of insulin resistance (25). The paradoxical elevation of plasma nesfatin-1 in subjects with T2DM might be a compensatory upregulation to compensate for the metabolic stress imposed by obesity. Alternatively, it is possible that obesity or T2DM may cause resistance to nesfatin-1 actions, leading to its compensatory upregulation. This scenario is reminiscent of hyperinsulinemia and hyperleptinemia, both of which are thought to be the consequence of increased production

in response to obesity associated insulin and leptin resistance. A similar elevation in obesity has also been reported in fibroblast growth factor-21, which is also thought to be a result of hormone resistance (26). However, the cross-sectional design of previous studies does not allow us to determine the cause-and-effect relationship between increased plasma nesfatin-1 level and T2DM. Indeed, there is still a paucity of information on the action of nesfatin-1 to influence glucose homeostasis. In particular, the contribution of central nesfatin-1 to glucose metabolism has not been systematically investigated. In this study, we investigated whether central nesfatin-1 directly affects hepatic and peripheral insulin sensitivity or results in improved insulin action via the changes associated signaling pathway. We show, for the first time to our knowledge, that central nesfatin-1 plays a role in controlling glucose metabolism via the TORC2/mTOR signaling pathway in insulin resistance conditions.
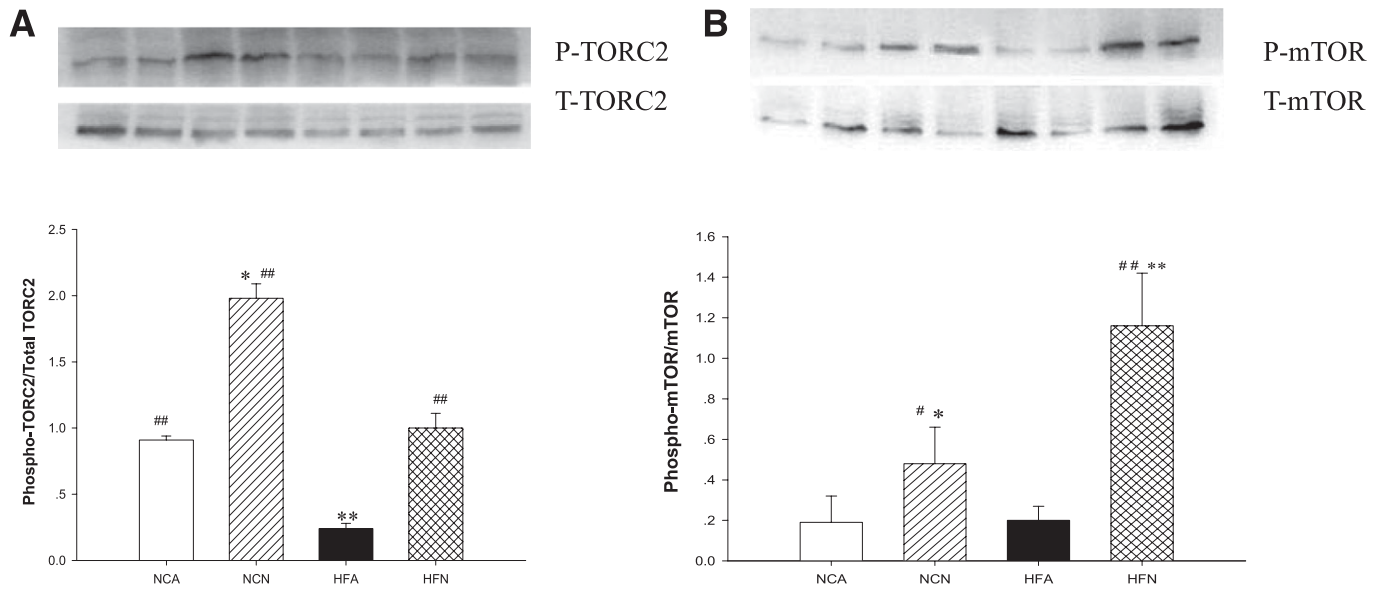
A

B

C

D
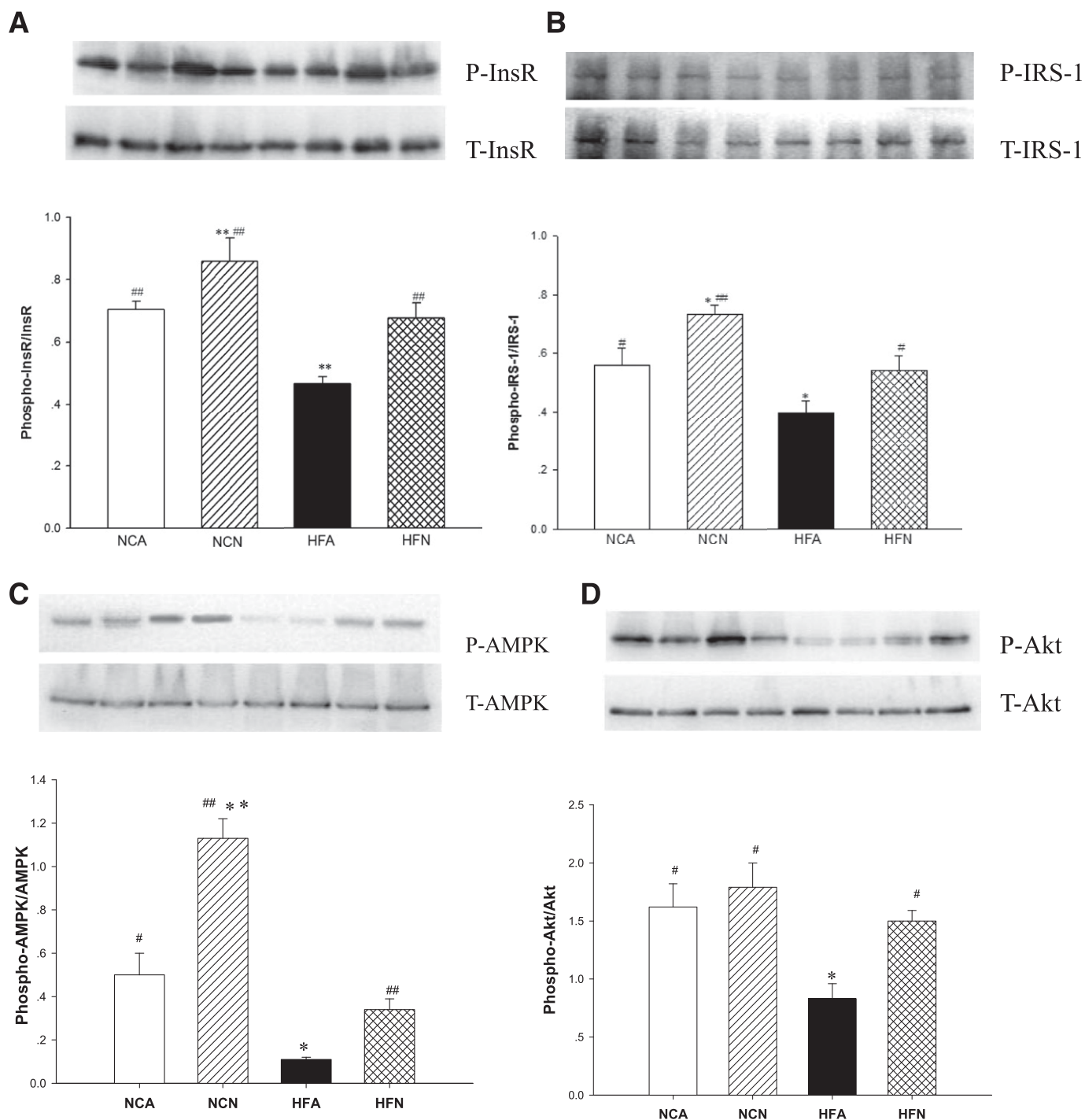
FIG. 5. Effect of ICV nesfatin-1 on liver insulin signaling pathway. Four treatment groups were studied: NCA, NCN, HFA, and HFN. Central nesfatin-1 administration markedly increased liver InsR (*A*), IRS-1 (*B*), AMPK (*C*), and Akt (*D*) phosphorylation in both SD- and HFD-fed rats. Ratio of phosphorylated vs. total protein was calculated and is shown as means ± SE (*n* = 5). *$P < 0.05$, **$P < 0.01$ vs. ICV ACF-infused rats (NCA), #$P < 0.05$, ##$P < 0.01$ vs. HFD-fed rats (HFA).

ICV infusion of nesfatin-1 in HFD-fed animals partially reversed the diet-induced insulin resistance by increasing insulin-mediated muscle glucose uptake and by suppressing HGP. It is well-known that insulin inhibits expression of PEPCK and G-6-Pase, two rate-limiting genes for gluconeogenesis. Thus, to further delineate the mechanisms by which central nesfatin-1 modulated glucose homeostasis, we assessed its contribution to gluconeogenesis by examining hepatic activity, mRNA, and protein levels of G-6-Pase

and PEPCK. We found that central nesfatin-1 resulted in a marked suppression of hepatic PEPCK mRNA and protein levels in both SD and HFD rats but failed to alter G-6-Pase activity and protein expression. Central nesfatin-1 appeared to antagonize the effect of HFD on increasing PEPCK gene expression in vivo. In agreement with decreasing PEPCK gene expression, central nesfatin-1 also resulted in a reduced PEPCK enzyme activity, further confirming that it affected PEPCK rather than G-6-Pase.

FIG. 6. Effect of ICV nesfatin-1 on liver TORC2 and mTOR (T-mTOR:Total-mTOR and P-mTOR:phospho-mTOR activation. Four treatment groups were studied: NCA, NCN, HFA, and HFN. Central nesfatin-1 administration markedly increased liver TORC2 (*A*) and mTOR (*B*) phosphorylation in both SD- and HFD-fed rats. Ratio of phosphorylated vs. total AMPK and Akt was calculated and is shown as means ± SE ($n = 5$). *$P < 0.05$, **$P < 0.01$ vs. ICV ACF-infused rats (NCA), #$P < 0.05$, ##$P < 0.01$ vs. HFD-fed rats (HFA).

The part of the glucose entering the liver is phosphorylated by glucokinase and then dephosphorylated by G-6-Pase. This futile cycle between glucokinase and G-6-Pase is named glucose cycling, and it accounts for the difference between the total flux through G-6-Pase and glucose production. G-6-Pase catalyzes the last step in both gluconeogenesis and glycogenolysis, and PEPCK is responsible only for gluconeogenesis. In this study, central nesfatin-1 led to a marked suppression of hepatic PEPCK protein and activity, but failed to alter hepatic G-6-Pase activity, suggesting that PEPCK may be more sensitive to short-term central nesfatin-1 exposure than G-6-Pase. In
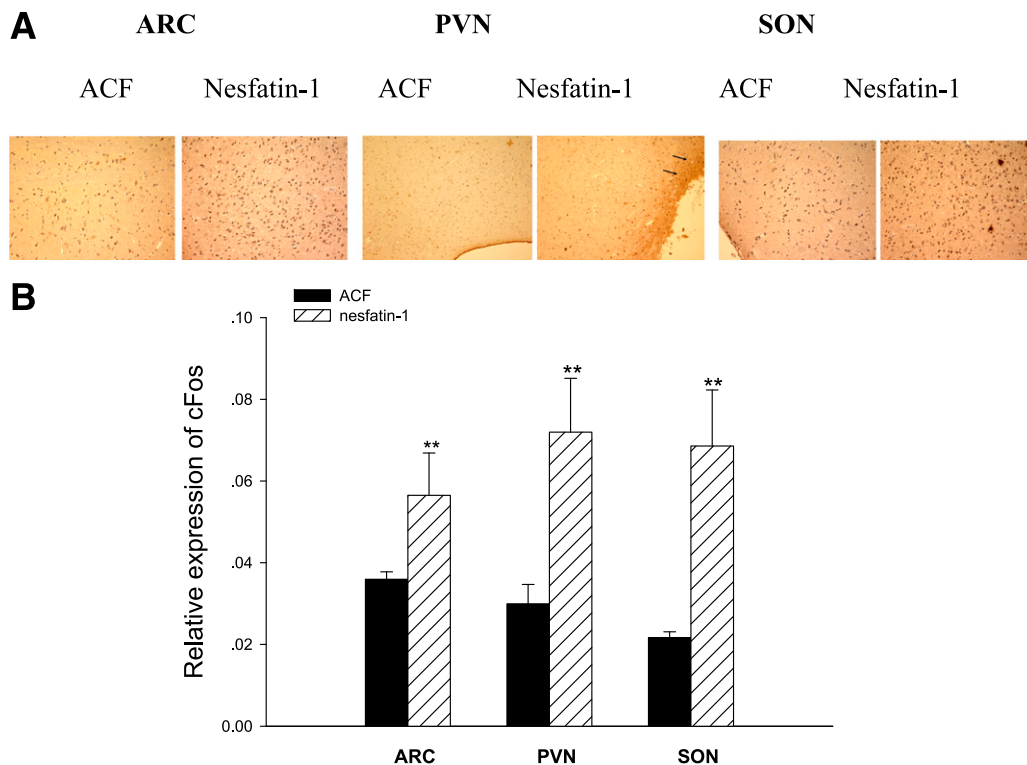
FIG. 7. Central nesfatin-1 stimulates Fos immunoreactivity (ir) in hypothalamic regions. *A*: Photomicrographs of coronal brain sections showing Fos immunostaining in the arcuate (ARC), paraventricular (PVN), and supraoptic nucleus (SON), after ICV nesfatin-1 or ACF treatment. Arrows illustrate that the number of Fos-positive cells was significantly greater. *B*: Number of Fos-ir cells per section in hypothalamic regions. Data are mean Fos-ir cells/hemisphere ± SEM; $n = 4$. **$P < 0.001$ vs. ACF. (A high-quality digital representation of this figure is available in the online issue.)

addition, we also considered that the suppression of HGP by central nesfatin-1 was dependent on an inhibition of the substrate flux through G-6-Pase and not on a decrease in the amount of G-6-Pase enzyme. Thus, in SD and HFD rats, central nesfatin-1 may have decreased glucose production mainly via decreasing gluconeogenesis and *PEPCK* activity.

Recently, it has been reported that ICV nesfatin-1 produced a dose-dependent delay of gastric emptying (27). To exclude that a decrease gastric emptying was responsible for the observed improvement in insulin sensitivity, rats were fasted for 12 h prior to experimentation and were not fed during the 6 h of the studies.

To further delineate the mechanism by which central nesfatin-1 modulates glucose homeostasis, we assessed the effects of central nesfatin-1 on the phosphorylation of several proteins in the InsR → IRS-1 → AMPK → Akt signaling cascade in the liver. We found that central nesfatin-1 significantly augmented InsR and IRS-1 tyrosine phosphorylation. These results demonstrated that central nesfatin-1 in both SD and HFD rats resulted in a stimulation of liver insulin signaling that could account for the increased insulin sensitivity and improving glucose metabolism.

AMPK is a key regulator of both lipid and glucose metabolism. It has been referred to as a metabolic master switch, because its activity is regulated by the energy status of the cell. In this study, we demonstrate that central nesfatin-1 resulted in increased phosphorylation of AMPK accompanied by a marked suppression of hepatic PEPCK activity, mRNA, and protein levels in both SD and HFD rats. Notably, central nesfatin-1 appears to prevent the obesity-driven decrease in phospho-AMPK levels in HFD-fed rats. Because hepatic AMPK controls glucose homeostasis mainly through the inhibition of gluconeogenic gene expression and glucose production (27), the suppressive effect of central nesfatin-1 on the HGP can be attributed partly to its ability to suppress the expression of PEPCK mRNA and protein through AMPK activation. Furthermore, the activation of AMPK has been shown to enhance glucose uptake in skeletal muscle (28,29). Therefore, increased AMPK phosphorylation by central nesfatin-1 may also have been responsible for the improved glucose uptake in muscle.

Akt is a key effector of insulin-induced inhibition of HGP and stimulation of muscle glucose uptake (30). We therefore examined the effects of central nesfatin-1 on Akt phosphorylation in vivo. We found that central nesfatin-1 produced a pronounced increase in insulin-mediated phosphorylation of Akt in the liver of HFD-fed rats. This increase was paralleled by an increase in muscle glucose uptake and inhibition of HGP. This provided correlative evidence that Akt activation may be involved in nesfatin-1 signaling and its effects on glucose homeostasis and insulin sensitivity.

The mTOR pathway has emerged as a molecular mediator of insulin resistance, which can be activated by both insulin and nutrients (31). It is needed to fully activate AKT and consists of two discrete protein complexes, TORC1 and TORC2, only one of which, TORC1, binds rapamycin. In addition to mTOR, the TORC2 complex contains rictor, mLST8, and SIN1 and regulates insulin action and Akt phosphorylation (31–34). Thus, mTOR sits at a critical juncture between insulin and nutrient signaling, making it important both for insulin signaling downstream from Akt and for nutrient sensing (35). Until now, it has not been known whether nesfatin-1 affects activation of mTOR.

To gain further insight into the mechanism underlying the insulin-sensitizing effects of ICV nesfatin-1, we assessed mTOR and TORC2 phosphorylation in liver samples of SD- and HFD-fed animals. Both mTOR and TORC2 phosphorylations were increased in livers from these rats, demonstrating activation of mTOR and TORC2 by central nesfatin-1 in vivo. As mTOR kinase activity is required for Akt phosphorylation (36–38), the observed increased Akt phosphorylation may have been caused by the concomitant activation of the mTOR/TORC2. Thus, we postulate that the mTOR/TORC2 plays a role as a negative-feedback mechanism in the regulation of metabolism and insulin sensitivity mediated by central nesfatin-1.

The mediobasal hypothalamus contains neuronal populations that mediate energy homeostasis. Immunohistochemistry of the immediate early gene Fos has been used to map neuronal targets of adipokines. For example, leptin induces intense Fos immunostaining in the arcuate and dorsomedial nuclei (22,39,40). To confirm whether this effect of central nesfatin-1 on liver glucose fluxes requires central signaling through hypothalamic nuclei, we examined Fos expression induced by ICV nesfatin-1 in the hypothalamic region. Central nesfatin-1 resulted in an increase of Fos immunoreactivity expression in the hypothalamic nuclei that mediate glucose homeostasis. This finding, combined with the glucose turnover data, suggests that central nerve innervation is required for mediating the effects of central nesfatin-1 on glucose metabolism.

In summary, our findings indicate that the ICV nesfatin-1 resulted in increased insulin signaling through Akt/AMPK/TORC2 and provide a potential mechanism for increased insulin sensitivity. Furthermore, an increased Fos expression by central nesfatin-1 in the hypothalamic nuclei suggests the importance of the neural pathway that links nesfatin-1 action in the brain to the regulation of glucose production in the liver. Most important, this study is the first to identify a neural-mediated pathway to explain how central nesfatin-1 affects glucose homeostasis.

REFERENCES

1. Székely M, Szelényi Z. Regulation of energy balance by peptides: a review. Curr Protein Pept Sci 2005;6:327–353
2. Kalra SP. Appetite and body weight regulation: is it all in the brain? Neuron 1997;19:227–230
3. Kalra SP, Dube MG, Pu S, Xu B, Horvath TL, Kalra PS. Interacting appetite-regulating pathways in the hypothalamic regulation of body weight. Endocr Rev 1999;20:68–100
4. Obici S, Feng Z, Morgan K, Stein D, Karkanias G, Rossetti L. Central administration of oleic acid inhibits glucose production and food intake. Diabetes 2002;51:271–275

5. Loftus TM, Jaworsky DE, Frehywot GL, et al. Reduced food intake and body weight in mice treated with fatty acid synthase inhibitors. Science 2000;288:2379–2381

6. Pocai A, Obici S, Schwartz GJ, Rossetti L. A brain-liver circuit regulates glucose homeostasis. Cell Metab 2005;1:53–61

7. Lam TK, Pocai A, Gutierrez-Juarez R, et al. Hypothalamic sensing of circulating fatty acids is required for glucose homeostasis. Nat Med 2005;11:320–327

8. Obici S, Feng Z, Arduini A, Conti R, Rossetti L. Inhibition of hypothalamic carnitine palmitoyltransferase-1 decreases food intake and glucose production. Nat Med 2003;9:756–761

9. Obici S, Rossetti L. Minireview: nutrient sensing and the regulation of insulin action and energy balance. Endocrinology 2003;144:5172–5178

10. El-Haschimi K, Pierroz DD, Hileman SM, Bjørbaek C, Flier JS. Two defects contribute to hypothalamic leptin resistance in mice with diet-induced obesity. J Clin Invest 2000;105:1827–1832

11. Münzberg H, Flier JS, Bjørbaek C. Region-specific leptin resistance within the hypothalamus of diet-induced obese mice. Endocrinology 2004;145:4880–4889

12. Van Heek M, Compton DS, France CF, et al. Diet-induced obese mice develop peripheral, but not central, resistance to leptin. J Clin Invest 1997;99:385–390

13. Clegg DJ, Benoit SC, Reed JA, Woods SC, Dunn-Meynell A, Levin BE. Reduced anorexic effects of insulin in obesity-prone rats fed a moderate-fat diet. Am J Physiol Regul Integr Comp Physiol 2005;288:R981–R986

14. Oh-I S, Shimizu H, Satoh T, et al. Identification of nesfatin-1 as a satiety molecule in the hypothalamus. Nature 2006;443:709–712

15. Brailoiu GC, Dun SL, Brailoiu E, et al. Nesfatin-1: distribution and interaction with a G protein-coupled receptor in the rat brain. Endocrinology 2007;148:5088–5094

16. Kohno D, Nakata M, Maejima Y, et al. Nesfatin-1 neurons in paraventricular and supraoptic nuclei of the rat hypothalamus coexpress oxytocin and vasopressin and are activated by refeeding. Endocrinology 2008;149:1295–1301

17. Ramanjaneya M, Chen J, Brown JE, et al. Identification of nesfatin-1 in human and murine adipose tissue: a novel depot-specific adipokine with increased levels in obesity. Endocrinology 2010;151:3169–3180

18. Li L, Yang G, Li Q, et al. Exenatide prevents fat-induced insulin resistance and raises adiponectin expression and plasma levels. Diabetes Obes Metab 2008;10:921–930

19. Li L, Yang G, Shi S, Yang M, Liu H, Boden G. The adipose triglyceride lipase, adiponectin and visfatin are downregulated by tumor necrosis factor-α (TNF-α) in vivo. Cytokine 2009;45:12–19

20. Thomas WM, Johnston IA. Starvation and the Activities of Glycolytic and Gluconeogenic Enzymes in Skeletal Muscles and Liver of the Plaice, Pleuronectes platessa. J Comp Physiol 1980;136:31–38

21. Davidson AL, Arion WJ. Factors underlying significant underestimations of glucokinase activity in crude liver extracts: physiological implications of higher cellular activity. Arch Biochem Biophys 1987;253:156–167

22. Elmquist JK, Ahima RS, Elias CF, Flier JS, Saper CB. Leptin activates distinct projections from the dorsomedial and ventromedial hypothalamic nuclei. Proc Natl Acad Sci USA 1998;95:741–746

23. Shimizu H, Oh-I S, Hashimoto K, et al. Peripheral administration of nesfatin-1 reduces food intake in mice: the leptin-independent mechanism. Endocrinology 2009;150:662–671

24. Stengel A, Goebel M, Yakubov I, et al. Identification and characterization of nesfatin-1 immunoreactivity in endocrine cell types of the rat gastric oxyntic mucosa. Endocrinology 2009;150:232–238

25. Zhang Z, Li L, Yang M, Liu H, Boden G, Yang G. Increased plasma levels of nesfatin-1 in patients with newly diagnosed type 2 diabetes mellitus. Exp Clin Endocrinol Diabetes 2012;120:91–95

26. Fisher FM, Chui PC, Antonellis PJ, et al. Obesity is a fibroblast growth factor 21 (FGF21)-resistant state. Diabetes 2010;59:2781–2789

27. Stengel A, Goebel M, Wang L, et al. Central nesfatin-1 reduces dark-phase food intake and gastric emptying in rats: differential role of corticotropin-releasing factor2 receptor. Endocrinology 2009;150:4911–4919

28. Hardie DG. AMP-activated/SNF1 protein kinases: conserved guardians of cellular energy. Nat Rev Mol Cell Biol 2007;8:774–785

29. Lee YS, Kim WS, Kim KH, et al. Berberine, a natural plant product, activates AMP-activated protein kinase with beneficial metabolic effects in diabetic and insulin-resistant states. Diabetes 2006;55:2256–2264

30. Yin J, Gao Z, Liu D, Liu Z, Ye J. Berberine improves glucose metabolism through induction of glycolysis. Am J Physiol Endocrinol Metab 2008;294:E148–E156

31. Cho H, Mu J, Kim JK, et al. Insulin resistance and a diabetes mellitus-like syndrome in mice lacking the protein kinase Akt2 (PKBβ). Science 2001;292:1728–1731

32. Sabatini DM. mTOR and cancer: insights into a complex relationship. Nat Rev Cancer 2006;6:729–734

33. Sarbassov DD, Guertin DA, Ali SM, Sabatini DM. Phosphorylation and regulation of Akt/PKB by the rictor-mTOR complex. Science 2005;307:1098–1101

34. Sarbassov DD, Ali SM, Sengupta S, et al. Prolonged rapamycin treatment inhibits mTORC2 assembly and Akt/PKB. Mol Cell 2006;22:159–168

35. Jacinto E, Facchinetti V, Liu D, et al. SIN1/MIP1 maintains rictor-mTOR complex integrity and regulates Akt phosphorylation and substrate specificity. Cell 2006;127:125–137

36. Fingar DC, Blenis J. Target of rapamycin (TOR): an integrator of nutrient and growth factor signals and coordinator of cell growth and cell cycle progression. Oncogene 2004;23:3151–3171

37. Corradetti MN, Guan KL. Upstream of the mammalian target of rapamycin: do all roads pass through mTOR? Oncogene 2006;25:6347–6360

38. Facchinetti V, Ouyang W, Wei H, et al. The mammalian target of rapamycin complex 2 controls folding and stability of Akt and protein kinase C. EMBO J 2008;27:1932–1943

39. Koo SH, Flechner L, Qi L, et al. The CREB coactivator TORC2 is a key regulator of fasting glucose metabolism. Nature 2005;437:1109–1111

40. Elias CF, Kelly JF, Lee CE, et al. Chemical characterization of leptin-activated neurons in the rat brain. J Comp Neurol 2000;423:261–281